Circular Kardar-Parisi-Zhang equation as an inflating, self-avoiding ring polymer

Silvia N. Santalla,[1] Javier Rodríguez-Laguna,[2,3] and Rodolfo Cuerno[3]

[1]*Departamento de Física and Grupo Interdisciplinar de Sistemas Complejos (GISC), Universidad Carlos III de Madrid, Leganés, Spain*
[2]*ICFO–Institut de Ciències Fotòniques, Castelldefels, Spain*
[3]*Departamento de Matemáticas and GISC, Universidad Carlos III de Madrid, Leganés, Spain*

We consider the Kardar-Parisi-Zhang equation for a circular interface in two dimensions, unconstrained by the standard small-slope and no-overhang approximations. Numerical simulations using an adaptive scheme allow us to elucidate the complete time evolution as a crossover between a short-time regime with the interface fluctuations of a *self-avoiding ring* or two-dimensional vesicle, and a long-time regime governed by the Tracy-Widom distribution expected for this geometry. For small-noise amplitudes, scaling behavior is only of the latter type. Large noise is also seen to *renormalize* the bare physical parameters of the ring, akin to analogous parameter renormalization for equilibrium three-dimensional membranes. Our results bear particular importance on the relation between relevant universality classes of scale-invariant systems in two dimensions.

PACS number(s): 81.15.Aa, 68.35.Ct, 05.10.Gg, 82.35.Gh

Recently, statistical fluctuations are revealing interesting features for a number of one-dimensional systems confined to circular geometries. For instance, for semiflexible polymers of a fixed length, such as constrained DNA rings, the closure condition influences the scaling, shape, and transport behavior [1]. Topology is actually expected to play a key role in a large number of related biophysical processes, such as, e.g., translocation in nanochannels or nanopores [2,3], or knot localization [4]. In particular, circular DNA molecules in two dimensions have been experimentally found [1] to be well described as pressurized vesicles [5], their scaling behavior depending on the geometry [6]. Thus, for deflated rings (negative pressure difference Δp), fluctuations are in the universality class of lattice animals, while for $\Delta p = 0$, statistics are those of a ring self-avoiding walk (SAW) [1]. The latter is important as a paradigmatic model of polymers [7] and because the SAW is believed to constitute a conformally invariant system in two dimensions [8].

For planar rings evolving far from equilibrium, the closure condition is also proving to be nontrivial, as recently observed in experiments with droplets of turbulent liquid crystals [9], for the edge of a drying colloidal suspension [10,11], and for many more systems, from epitaxy to bacterial growth [12]. Thus, as proposed in Ref. [13], the probability distribution function (PDF) of the height fluctuations for interfaces which, as many of these, belong to the Kardar-Parisi-Zhang (KPZ) universality class [14,15], depends on the global curvature. The eponymous equation [16], which is the prime representative for these systems, is a continuum model for the evolution of a rough interface between a (stable, e.g., solid) phase that grows at the expense of a (an unstable, e.g., vapor) phase,

$$\partial_t h = v + \nu \nabla^2 h + \frac{\lambda}{2}(\nabla h)^2 + \eta(\mathbf{x},t), \qquad (1)$$

where $h(\mathbf{x},t)$ is the height field above the substrate position $\mathbf{x} \in \mathbb{R}^d$ at time t, η is Gaussian white noise, v is the growth speed for a flat interface, and $\nu > 0$, λ are additional parameters. On the one hand, from the point of view of the theory of stochastic processes, the KPZ equation features a remarkable example of a time crossover [17,18] between the two main universality classes of kinetic roughening [14,15], namely, the

Edwards-Wilkinson (EW) class at short times, and the KPZ class at long times. Experimentally [9], however, while such a crossover may have been seen in $d = 1$ for interfaces with a null global curvature, it has not for the circular geometry case. On the other hand, for such ring-shaped interfaces, height statistics are indeed distinctively described [13] by the Tracy-Widom (TW) PDF for the largest eigenvalue of large random matrices in the Gaussian unitary ensemble (GUE), as recently supported by exact solutions of the KPZ equation on an infinite substrate and a wedge initial condition (but without explicit closure), or for related systems [19]. This actually occurs with a remarkable degree of universality [17,20], as the same PDF, critical exponents, and limiting processes apply to discrete models, continuum equations [21], and experiments [9–11]. Hence, in two dimensions (2D) both pressurized vesicles and the KPZ equation notably demonstrate the nontrivial role of geometry, as a part of the universality class and related renormalization-group fixed point [6], in and out of equilibrium, respectively.

Note, Eq. (1) is just the small-slope, single-valued approximation of a more general equation [22],

$$\partial_t \mathbf{r} = [A_0 + A_1 K(\mathbf{r}) + A_n \eta(\mathbf{r},t)] \mathbf{u}_n, \qquad (2)$$

where $\mathbf{r}(t) \in \mathbb{R}^{d+1}$ gives the interface position, $K(\mathbf{r})$ is the local extrinsic surface curvature, $\mathbf{u}_n$ is the normal direction pointing towards the unstable phase, and constants A_0, A_1, and A_n relate to parameters in Eq. (1) in a simple way [22]. They account for, respectively, the average growth speed along the local normal direction, surface tension effects, and noise in the local growth velocity, precisely the physical mechanisms at play in the formulation of the KPZ equation as a continuum interface model [16]. However, those produced by Eq. (2) are not constrained to small slopes or lack of overhangs [22].

For a ring geometry and $d = 1$, Eq. (1) actually has to be given up in favor of Eq. (2), since the closure condition hinders description of the interface profile by a single-valued function altogether. Alternative formulations to Eq. (2) are available (see, e.g., in Ref. [12]), although most include the neglect of overhangs and/or additional simplifications. A natural question is then whether Eqs. (1) and (2) have the same

dynamic scaling properties. Here we show that, for planar rings, this is *not* the case. Namely, while asymptotics are indeed of the expected TW-GUE type also for Eq. (2), which implements explicitly a closure condition, the early times differ substantially as compared to Eq. (1): Now, for small-noise amplitudes no scaling behavior other than KPZ is obtained, as in experiments [9], while 2D SAW universality is obtained at short times for large-noise amplitude values A_n. Such large fluctuations renormalize additional parameters such as A_1, in a form that is reminiscent of surface tension renormalization by nonequilibrium fluctuations, as experimentally assessed, e.g., in Ref. [23] for three-dimensional (3D) active membranes. In parallel with the equilibrium behavior of 2D vesicles [6] as a function of Δp, the change from early-time SAW to late-time KPZ scaling behavior correlates with an evolution in time from a freely fluctuating ring to an average circular shape. Thus, the generalized KPZ equation (2) also predicts a crossover to occur during the time evolution of the system between two equally celebrated universality classes under large-noise conditions. From this point of view the experiments in Ref. [9] correspond to a small-noise condition, while a prediction is provided for suitable large-noise situations, which should be amenable to experimental verification.

We have performed numerical simulations of Eq. (2) using planar rings of various initial radii R_0 and center $(0,0)$ as initial conditions. We employ an adaptive algorithm as in Refs. [22,24], which does not need to assume a single-valued polar function. The interface is represented by a chain of points (a "polymer") $\{P_i\}_{i=1}^{N(t)} \subset \mathbb{R}^2$ defining a piecewise continuous curve which always leaves the stable phase on its left. The distance between them is forced to remain in an interval $[l_{min}, l_{max}]$, which is achieved by inserting or removing points dynamically. Interface properties, such as curvature, are evaluated in a geometrically natural way [22]. Unavoidably, self-intersections occur along the evolution. We always remove the smaller interface component, eliminating both cavities and outgrowths, thus implementing self-avoidance and rendering the dynamics irreversible. This approximation is akin to restricting dynamics to that of the active zone in growth

systems [22]. Time updates are via a Euler-Maruyama scheme with spacing Δt, sufficiently small that it does not appreciably influence results.

A set of representative snapshots are shown in Fig. 1, for $R_0 = 10$, $A_0 = 0.01$, $A_1 = 0.01$, $A_n = 1$, and different times. Qualitatively, the ring can be seen to undergo two different regimes: (I) For $t \lesssim 100$ it fluctuates without significant growth while its shape becomes less and less circular; (II) for $t \gtrsim 400$, the ring grows steadily, progressively recovering an average circular shape. In order to interpret these observations, we can consider the deterministic case, i.e., $A_n = 0$. Rings with smaller R_0 than a certain threshold shrink, since the constant average velocity A_0 is not able to compensate for the effect of surface tension A_1. On the other hand, for $R_0 \gtrsim A_1/A_0$, the ring grows very slowly at first, and with velocity A_0 for longer times.

From Eq. (2), a simplified evolution equation can be derived for the average ring radius $R(t)$,

$$\frac{dR(t)}{dt} = \tilde{A}_0 + \frac{\tilde{A}_1}{R(t)}, \qquad (3)$$

where local variations in the normal velocity are neglected and the total ring length $L(t)$ is approximated by that of the average circle (see details in Ref. [25]). Here, $\tilde{A}_{0,1}$ have values that will in general differ from their "bare" counterparts $A_{0,1}$ due to noise-induced renormalization. Figure 2 shows $R(t)$ for the same parameter choice of Fig. 1. Regimes I and II are clearly distinguished in the growth rate. Remarkably, the numerical $R(t)$ fits the *exact* solution of Eq. (3) [25] for $\tilde{A}_0 \approx 0.026 > 0.01 = A_0$ and $\tilde{A}_1 \approx 0.1 > 0.01 = A_1$. For small-noise amplitudes, no such noise renormalization occurs (see Ref. [25]). Thinking of A_0 as a *pressure difference* that attempts to "inflate" the ring [5,6], the effect of A_n can be thought of as a *fluctuation-induced* pressure boost $\tilde{A}_0$. Alongside, $\tilde{A}_1$ becomes an enhanced surface tension, due to the noisy dynamics. Similar fits are obtained for a wide range of bare parameters.

Figure 2(a) also depicts the numerical evolution of the actual $L(t)$ (for a space cutoff l_{min}). Very early in regime
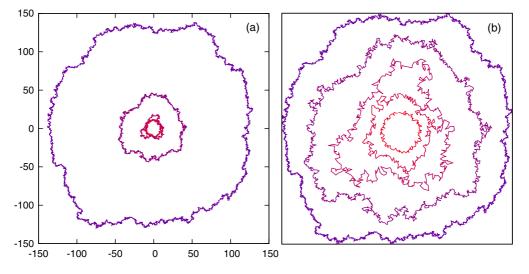

FIG. 1. (Color online) (a) Interface evolution for $R_0 = 10$, $A_0 = 0.01$, $A_1 = 0.01$, and $A_n = 1$, with $\Delta t = 0.1$, $l_{min} = 0.1$, and $l_{max} = 1$. Curves for times $t = 2, 20, 150, 1000$, and 5000, inner to outer. (b) Rescaled view to ease comparison. All units are arbitrary.
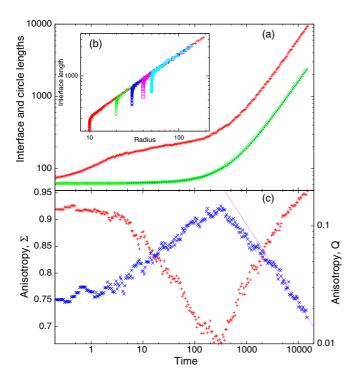
FIG. 2. (Color online) Evolution of *interface shape* for the case shown in Fig. 1. (a) Interface length (above) and circle length $2\pi R(t)$ (below), with $R(t)$ the fitted radius vs time. For long times, both are linear in t. Dashed line: Fit to a renormalized deterministic growth. (b) Interface length vs radius for different initial radii, $R_0 = 10, 20, 30, 40,$ and 50 (growing upwards). (c) Anisotropy vs time: Σ (+), left vertical axis, and quadrupole moment Q ($\times$), right vertical axis. The slope of the straight line, -0.667, corresponds to a fit for long times. Units are arbitrary.

I, while the average radius remains almost constant, this length increases due to fluctuations. In regime II, when $R(t)$ grows steadily, $L(t)$ actually becomes proportional to it. This behavior is appreciated in Fig. 2(b), where the $L(t)$ is plotted versus $R(t)$. There is a threshold total length, proportional to R_0, below which no radial growth occurs, and above which both measures become proportional. As seen in Fig. 1, prior to regime II, noise basically induces loss of the initial circular symmetry. In Fig. 2(c) we quantify this effect by plotting the asymmetry parameter [26] $\Sigma(t) = \langle S_{G1}^2/S_{G2}^2 \rangle$, i.e., the ratio of the smallest to largest eigenvalues, S_{G1}^2, S_{G2}^2, of the gyration tensor S. This is frequently used to assess polymer classes in terms of self-avoidance, dimensionality, rigidity, etc [1,6,27,28]. In our case, $\Sigma(t)$ decreases with time, reaches a minimum value $\Sigma(t \simeq 400) \simeq 0.68$, and increases back, approaching the characteristic value of a circular swollen polymer in regime II. Other measures of anisotropy lead to the same conclusion [see, e.g., Fig. 2(c) for the quadrupole moment, $Q^2 = \langle |x^2 - y^2| \rangle / \langle r^2 \rangle$, where x, y, and r are relative to the center of mass (CM) of the $\{P_i\}_{i=1}^{N(t)}$ point distribution].

Given the relevance of fluctuations in these dynamics, we assess them in Fig. 3(a), where we show the time evolution of the global interface roughness, $W_{CM}(t) = \langle [P_i(t) - R_{CM}(t)]^2 \rangle^{1/2}$, with $R_{CM}(t)$ being the position of the CM [29]. Scaling behavior $W(t) \sim t^\beta$ holds, with $\beta \simeq 1/3$, *both* in regimes I and II. As standard for kinetic roughening systems
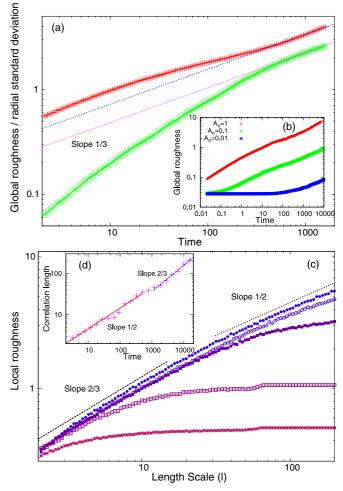

FIG. 3. (Color online) Evolution of the *interface fluctuations* for the case shown in Fig. 1. (a) Global roughness (+) and standard deviation of $R(t)$ ($\times$) vs time. Both straight lines have slopes 1/3. (b) $W(t)$ for decreasing noise amplitude, as in the legend, top (same data as in the main panel) to bottom. (c) Local roughness vs window size, for $t = 2, 20, 1200, 8000,$ and $14\,000$, bottom to top. Straight lines have slopes as in the legend. (d) Correlation length vs time. Straight lines have slopes 1/2 (lower left corner) and 2/3 (upper right corner). All units are arbitrary.

in a circular geometry, $W(t)$ does not saturate due to the uninterrupted growth of the system size [30]. Moreover, as indicated in Fig. 2(c), during regime II the quadrupole moment Q decays as $t^{-2/3}$, which follows if we estimate Q as the ratio of the radial fluctuations to the average radius, $t^{\beta-1} \approx t^{-2/3}$. We also measure the local roughness $w(l,t)$, namely, the interface fluctuations (restricted to windows of size l) around a fitting circular arc, which is drawn with respect to the CM. Data are shown in Fig. 3(c) as functions of l, for several times. Scaling behavior ensues, $w(l) \sim l^\alpha$, provided that, as in the standard Family-Vicsek (FV) ansatz [14], the window size l is smaller than a correlation length $\xi(t)$, which itself grows as $\xi(t) \sim t^{1/z}$. The FV scaling relation $z = \alpha/\beta$ holds for exponent values (α, z) which are $(2/3, 2)$ in regime I, and $(1/2, 3/2)$ in regime II [see Fig. 3(d)]. Indeed, in both cases $\beta = 1/3$, as implied by $W(t)$. Hence, the fractal dimension $D_F = 2 - \alpha$ [14] changes from 4/3 in regime I to 3/2 in regime II. Overall, the evolution is from kinetic
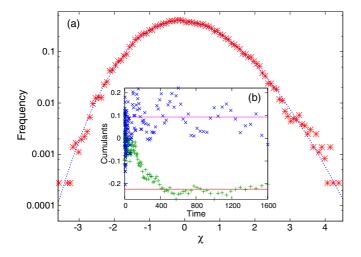
FIG. 4. (Color online) (a) Histogram of rescaled radial fluctuations χ at late times $t \in [700,1500]$ for the case shown in Fig. 1. Simulation data (∗) and analytic TW-GUE distribution (dashed line). (b) Time evolution of skewness (lower, +) and kurtosis (upper, ×) of $R(t)$ for numerical data, with the analytic values for the TW-GUE distribution as solid lines. Due to a negative Γ in Eq. (4), the skewness converges to *minus* the value for the TW-GUE distribution. All units are arbitrary.

roughening in the SAW class (regime I), for which $\alpha_{\mathrm{SAW}} = 2/3$ [7] and $\beta_{\mathrm{SAW}} = 1/3$ [31,32], to asymptotic KPZ scaling in regime II, for which $\alpha_{\mathrm{KPZ}} = 1/2$ and $\beta_{\mathrm{KPZ}} = 1/3$ [14]. If the noise amplitude decreases significantly ($A_n \lesssim 0.01$), the roughness remains constant in regime I, namely, the SAW stage disappears, the only measurable scaling behavior being the KPZ asymptotics in regime II, as in the experiments for circular geometry [9]. See Fig. 3(b).

The progressive dominance of radial fluctuations can be appreciated in Fig. 3(a), where we plot the time evolution for the standard deviation of the random variable $R(t)$. Although this quantity grows fast with t, numerically it remains much smaller than $W(t)$ until the onset of regime II, after which both remain proportional. Actually, we can further explore radial fluctuations in the asymptotic KPZ regime. Thus, following Prähofer and Spohn [13], we rewrite

$$R(t) \approx \rho_0 + Vt + \Gamma t^\beta \chi, \qquad (4)$$

where ρ_0, V, and Γ are constants, $\beta = \beta_{\mathrm{KPZ}}$, and χ is a random variable with zero average and unit variance, whose probability distribution is stationary and corresponds to the TW-GUE distribution [9–11,13,19]. We have collected the instantaneous radii data for 17 different times in the range $t \in [700,1500]$, i.e., well within regime II, for 2500 noise realizations, in order to check this conjecture. Results are shown in Fig. 4(a), where we plot the probability distribution of χ, obtained following the procedure described in Ref. [33], and compare it with the analytical result [17]. Moreover, we have measured the third and fourth cumulants of this χ distribution, i.e., the skewness and kurtosis, which are, respectively, $\langle\chi^3\rangle_c \approx 0.233$

and $\langle\chi^4\rangle_c \approx 0.0733$. The theoretical values for the TW-GUE distribution are [13] 0.224 for the skewness and 0.093 for the kurtosis, which are close enough. For comparison [13], for the TW-GUE distribution, the skewness is 0.293 and the kurtosis 0.165, both being zero for the Gaussian distribution. Figure 4(b) shows the time evolution of the cumulants of $R(t)$ towards the TW-GUE values. We must remark on the *negative* sign that we obtain for parameter Γ in Eq. (4), implying a negative skewness for $R(t)$. Physically, this is due to the fact (data not shown) that, in regime II, the number of cavities removed per unit length and unit time by the self-intersection removal condition is smaller than the number of removed outgrowths.

In summary, while for relatively small noise, perhaps as the experimentally studied case [9], only KPZ scaling is obtained, for large-noise intensities Eq. (2) predicts a circular interface to cross over in time between an early-time SAW regime, in which it behaves as a freely fluctuating ring "polymer," and the late-time regime controlled by KPZ fluctuations in the presence of nonzero average curvature. For small times, the local driving does not suffice to counteract fluctuations, so that the average circular shape smears out, interactions among interface points being controlled by surface tension (note the dynamic exponent indeed is $z = 2$ in regime I). Since $\xi(t)$ increases while $R(t)$ stays almost constant, eventually the system becomes fully correlated. From that time on, the increasing length needs to be accommodated in the finite area enclosed by the initial radius, and the intersection removal mechanism becomes relevant, smoothing out the interface. Because of the average (convex) circular geometry, cavities are removed more frequently than outgrowths, and the interface starts to grow, leading to the expected KPZ regime, with TW-GUE characteristics.

Our results conspicuously connect the celebrated 2D SAW and KPZ universality classes, both of which underscore the importance of geometrical constraints for scaling behavior, in and out of equilibrium. Crucially, the transition in time between them can only be elucidated through the existence of overhangs, which eludes other *continuum* models of kinetic roughening. Hence, the large-noise regime I of Eq. (2) might constitute a scaling limit for the 2D ring SAW [8], while providing an efficient algorithmic procedure to generate them [34]. Alternative connections between the KPZ and SAW classes are available, namely, between isoheight lines of the 2+1 dimensional (3D) KPZ equation and 2D SAW-related formulations [35]. In general, the conformation and dynamics of circular polymers are still subjects of considerable interest [36]. Current experimental capabilities reach even down to single molecule experiments [1], so that one might speculate on the possibility to observe a dynamical transition of the type elucidated here in appropriate nonequilibrium, 2D constrained settings [37].

[1] G. Witz, K. Rechendorff, J. Adamcik, and G. Dietler, Phys. Rev. Lett. **106**, 248301 (2011).

[2] C. Micheletti and E. Orlandini, Macromolecules **45**, 2113 (2012).

[3] K. Luo, T. Ala-Nissila, S.-C. Ying, and A. Bhattacharya, Phys. Rev. Lett. **100**, 058101 (2008).

[4] E. Ercolini *et al.*, Phys. Rev. Lett. **98**, 058102 (2007).

[5] S. Leibler, R. R. P. Singh, and M. E. Fisher, Phys. Rev. Lett. **59**, 1989 (1987).

[6] C. J. Camacho and M. E. Fisher, Phys. Rev. Lett. **65**, 9 (1990).

[7] J. des Cloizeaux and G. A. Jannink, *Polymers in Solution, Their Modelling and Structure* (Oxford University Press, Oxford, U.K., 1990).

[8] J. L. Cardy, Adv. Phys. **318** (2005); M. Bauer and D. Bernard, Phys. Rep. **432**, 115 (2006); I. A. Gruzberg, J. Phys. A: Math. Gen. **39**, 12601 (2006).

[9] K. A. Takeuchi and M. Sano, Phys. Rev. Lett. **104**, 230601 (2010); K. A. Takeuchi, M. Sano, T. Sasamoto, and H. Spohn, Sci. Rep. **1**, 34 (2011); K. A. Takeuchi and M. Sano, J. Stat. Phys. **147**, 853 (2012); K. A. Takeuchi, Phys. Rev. Lett. **110**, 210604 (2013).

[10] P. Yunker *et al.*, Phys. Rev. Lett. **110**, 035501 (2013); **111**, 209602 (2013).

[11] M. Nicoli, R. Cuerno, and M. Castro, Phys. Rev. Lett. **111**, 209601 (2013).

[12] Y. Saito, M. Dufay, and O. Pierre-Louis, Phys. Rev. Lett. **108**, 245504 (2012).

[13] M. Prähofer and H. Spohn, Phys. Rev. Lett. **84**, 4882 (2000); Physica A **279**, 342 (2000).

[14] A.-L. Barabási and H. E. Stanley, *Fractal Concepts in Surface Growth* (Cambridge University Press, Cambridge, U.K., 1995).

[15] J. Krug, Adv. Phys. **46**, 139 (1997).

[16] M. Kardar, G. Parisi, and Y.-C. Zhang, Phys. Rev. Lett. **56**, 889 (1986).

[17] I. Corwin, Random Matrices: Theor. Appl. **1**, 1130001 (2012).

[18] T. Gueudre, P. Le Doussal, A. Rosso, A. Henry, and P. Calabrese, Phys. Rev. E **86**, 041151 (2012).

[19] T. Sasamoto and H. Spohn, Phys. Rev. Lett. **104**, 230602 (2010); G. Amir, I. Corwin, and J. Quastel, Commun. Pure Appl. Math. **64**, 466 (2011).

[20] T. Kriecherbauer and J. Krug, J. Phys. A: Math. Theor. **43**, 403001 (2010).

[21] S. G. Alves, T. J. Oliveira, and S. C. Ferreira, Europhys. Lett. **96**, 48003 (2011); T. J. Oliveira, S. C. Ferreira, and S. G. Alves, Phys. Rev. E **85**, 010601(R) (2012).

[22] J. Rodríguez-Laguna, S. N. Santalla, and R. Cuerno, J. Stat. Mech.: Theor. Exp. (2011) P05032.

[23] M. D. El Alaoui Faris, D. Lacoste, J. Pécréaux, J.-F. Joanny, J. Prost, and P. Bassereau, Phys. Rev. Lett. **102**, 038102 (2009).

[24] S. Iv. Blinnikov and P. V. Sasorov, Phys. Rev. E **53**, 4827 (1996).

[25] See Supplemental Material at http://link.aps.org/supplemental/10.1103/PhysRevE.89.010401 for further details on Eqs. (2) and (3), and the simulation and measurement procedures that we have employed.

[26] F. Family, T. Vicsek, and P. Meakin, Phys. Rev. Lett. **55**, 641 (1985).

[27] M. Bishop and C. J. Saltiel, J. Chem. Phys. **85**, 6728 (1986).

[28] K. Alim and E. Frey, Phys. Rev. Lett. **99**, 198102 (2007).

[29] We have verified that—in contrast with cases such as the Eden model [see S. C. Ferreira, Jr. and S. G. Alves, J. Stat. Mech. (2006) P11007]—measurements of the roughness with respect to a fixed point instead of the CM do not change results on critical exponent values.

[30] J. M. Pastor and J. Galeano, Central Eur. J. Phys. **5**, 539 (2007).

[31] D. Stauffer and N. Jan, Can. J. Phys. **66**, 187 (1988).

[32] P. Devillard, Physica A **153**, 189 (1988).

[33] To obtain the histogram for χ, we follow a procedure similar to Ref. [9]. Namely, the raw (t, R) pairs are fit to a linear function of time, providing ρ_0 and V. The squared residuals are fit to a power law of time, yielding $|\Gamma|$ and $\beta \approx 0.3353$. From here we estimate the values $\chi = (R - \rho_0 - Vt)/(\Gamma t^{\beta})$. Finally, Γ has the same sign as the skewness of $R(t)$.

[34] E. J. Janse van Rensburg, J. Phys. A: Math. Theor. **42**, 323001 (2009).

[35] A. A. Saberi and S. Rouhani, Phys. Rev. E **79**, 036102 (2009).

[36] R. M. Robertson, S. Laib, and D. E. Smith, Proc. Natl. Acad. Sci. USA **103**, 7310 (2006).

[37] Y. Oh, H. W. Cho, J. Kim, C. H. Park, and B. J. Sung, Bull. Korean Chem. Soc. **33**, 975 (2012).